# Tangential Interface Stiffness Estimation of Dry-Joint Masonry Structures Through an Extended Experimental Campaign

Carla Colombo, Georgios Vlachakis, Christiam C Angel, Anastasios I Giouvanidis, Nathanaël Savalle, Nuno Mendes, Paulo B Lourenc

# Tangential interface stiffness estimation of dry-joint masonry structures through an extended experimental campaign

Carla Colombo [a]*, Georgios Vlachakis [a], Christiam C. Angel [a], Anastasios I. Giouvanidis [a], Nathanaël Savalle [b], Nuno Mendes [a], and Paulo B. Lourenço [a]

[a] University of Minho, ISISE, Department of Civil Engineering, Guimarães, Portugal. (***corresponding author***)

[b] Université Clermont Auvergne, Clermont Auvergne INP, CNRS, Institut Pascal, F-63000 Clermont-Ferrand, France

**Abstract**:

Many monumental masonry structures, such as aqueducts and public or military constructions, have been built using regular units neatly dressed without mortar. Detailed numerical modeling is commonly utilized to simulate the behavior of such dry-joint structures, which necessitates the proper definition of various physical and mechanical input parameters to enhance the reliability of the results. Among them, the normal and tangential interface stiffness play a key role in simulating masonry (either mortared or dry-joint) structures. Despite their paramount importance, the existing literature lacks established experimental studies for their characterization, and importantly their comparative validation. To this end, this paper presented an extensive experimental campaign on limestone blocks focusing on the estimation of the tangential interface stiffness. Two intrinsically different methodologies were employed for the tangential interface stiffness description, aiming to obtain reliable and cross-validated results. The first methodology, namely deformation-based, used direct shear-box tests and measured the interface shear deformation upon shear stresses for different levels of normal stress. The second methodology, namely vibration-based, utilized ambient vibration noise to measure the natural frequencies of the dry-stack assembly, which was correlated with the tangential interface stiffness through an inverse dynamic analysis. The dependence of the tangential interface stiffness with respect to the normal stress acting at the interface was discussed and the two methodologies were compared and validated.

**Keywords**: Tangential interface stiffness, dry-joint, masonry structures, contact mechanics, deformation-based tests, vibration-based tests

# 1 Introduction

The use of masonry as a building material is broadly spread all over the world, and its wide presence includes geographical areas threatened by earthquakes (Sorrentino et al. 2019). Post-earthquake surveys highlighted the high risk associated with masonry construction, consequently calling the need for their preservation (Vlachakis et al. 2020). Within the extended list of masonry structure typologies, dry-joint masonry is particularly vulnerable to seismic action, although extensively adopted as a construction technique, including constructions of relevant architectural heritage value (Roca et al. 2019). In addition, many historical masonry structures initially assembled with very thin layers of weak mortar have experienced mortar erosion and lixiviation, resulting in a structural behavior similar to dry-joint systems.

The research community demonstrates significant effort in assessing the seismic behavior of masonry structures with numerical or analytical models, which however require a notable number of input parameters coming from experimental campaigns (D'Altri et al. 2019). The reliable assessment of the dynamic behavior of dry-joint masonry structures necessitates an accurate description of the contact between the units (Colombo et al. 2022, Galvez et al. 2022, Al Shawa et al. 2012, Vlachakis et al. 2021). Among the studies devoted to the characterization of the contact properties, the ones committed to the interface stiffness estimation are limited, especially in the masonry community, and non-regulated by standardized experimental procedures. Nevertheless, in the scientific literature of different engineering fields, three categories of experimental methods are identified: i) deformation-based (Bandis et al. 1983, Berthoud and Baumberger 1998, Filippi et al. 2004, Kartal et al. 2011, Kulatilake et al. 2016), ii) vibration-based (Gimpl et al. 2022, Kim et al. 2021, Shi and Polycarpou 2005, Zhao et al. 2018), and wave-based (Baltazar et al. 2002, Drinkwater et al. 1996, Dwyer-Joyce et al. 2001, Mulvihill et al. 2013, Pesaresi et al. 2020). The deformation-based method directly estimates the interface stiffness by measuring the interface deformation upon loading, while the vibration-based method indirectly correlates the interface stiffness with the dynamic properties of the system, i.e. the frequencies of vibration and the mode shapes. Finally, the wave-based method correlates the interface stiffness with properties related to waves emitted through bodies separated by a joint. Despite the existence of several methods, just a few studies aimed at comparing the outcomes among them. Additionally, the outcomes of these studies showed relevant discrepancies between the methods, therefore lacking cross-validated results (Fantetti et al. 2021, Gimpl et al. 2022, Mulvihill et al. 2013).

This study presents an experimental campaign on the investigation of the tangential interface stiffness of dry-joint limestone specimens. Two experimental methods are employed, namely deformation-based and vibration-based. The behavior of the tangential interface stiffness is estimated for a large range of acting normal stress, successfully cross-validating the results of the two experimental methods.

# 2 Experimental Campaign

## 2.1 Material and specimens

The experimental study adopts limestone parallelepiped blocks of different dimensions, which vary according to the experimental method. The deformation-based tests, i.e. shear-box tests described in the following sub-section 2.2, consider seven squared specimens of dimension 58.5 mm (CoV=1.5 %, N=7) in the base/width, and 27.7 mm (CoV=13.1 %, N=7) in height (Figure 1a). Figure 1b shows five representative limestone specimens adopted for the vibration-based tests (described in sub-section 2.3). All the specimens have the same base dimension, equal to 49.9 mm (CoV=1.7 %, N=60) in width and

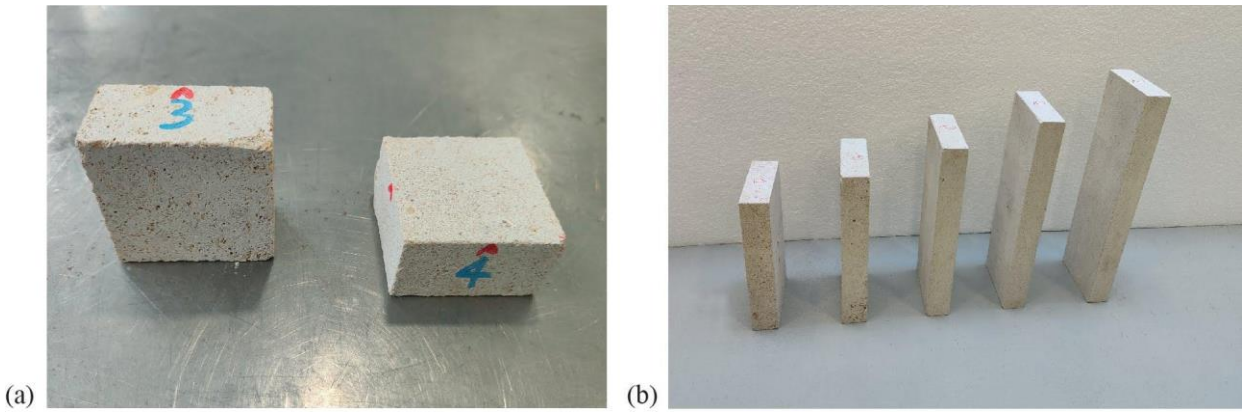


**Figure 1.** Limestone specimens adopted for: **(a)** the shear-box tests, and **(b)** the vibration-based tests with increasing height

150.8 mm (CoV=0.5 %, N=60) in length, while their height ranges from 200 mm to 750 mm, with a constant step of 50 mm. The specimens are 60 in total, forming 12 groups of 5 identical blocks.

The limestone units have a density of $\rho_{stone}$=2237.7 kg/m$^3$. The compressive strength $f_c$ and the elastic modulus $E$ of the material were determined by performing five uniaxial compression tests on limestone cylinders of 69.6 mm (CoV=0.0 %, N=5) radius and 178.5 mm (CoV=1.1 %, N=5) height (ASTM D7012-14E1 2017). An average compressive strength equal to 47.6 MPa (CoV=7.9 %, N=5) was obtained, while the elastic modulus $E_{stone}$ is estimated equal to 32.7 GPa (CoV=4.7 %, N=5), by applying a load up to ⅓ of $f_c$.

## 2.2 Deformation-based Tests

The tangential interface stiffness can be characterized using the deformation-based experimental strategy. The method consists of applying a constant pre-compression normal stress $\sigma_n$, while imposing and measuring the tangential stress $\tau_s$ and the tangential relative displacement $u_{j,s}$ (Figure 2a). The tangential interface stiffness $k_s$ is estimated as the gradient of the tangential stress $\tau_s$ with respect to the tangential displacement $u_{j,s}$ as follows:

$$k_s = \frac{d\tau_s}{du_{j,s}} \tag{1}$$

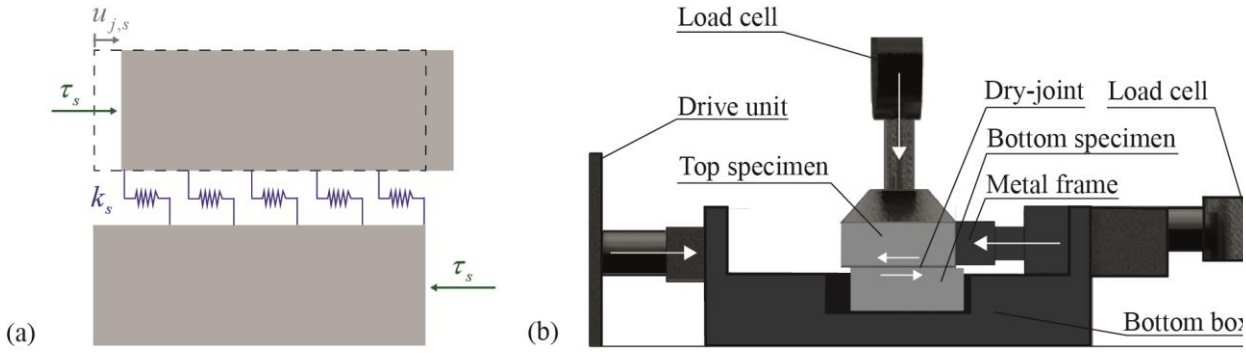


**Figure 2. (a)** Illustration of the interface behavior upon shear stress and **(b)** scheme of the shear-box experimental setup

The experimental setup employs a shear-box apparatus, whose components are illustrated in Figure 2b. In detail, a bottom limestone squared specimen is located in the bottom box, while another specimen is placed on top, bounded by a metal frame, forming the dry-joint under investigation. The shear-box test is guided by a drive unit that imposes the constant normal stress on the top specimen and the horizontal displacement on the bottom specimen. The vertical and horizontal load cells record the vertical and horizontal forces, while a Digital Image Correlation (DIC) system captures the relative tangential displacement at the joint. The DIC system allows recording purely the relative displacement at the interface, disregarding any possible additional flexibility, i.e. due to the unit and/or apparatus flexibilities (Kartal et al. 2011). Ten different pairs of specimens are tested considering 20 different normal pre-compression levels, i.e. from 0.004 MPa to 1 MPa, and assuming a constant velocity of 0.1 mm/min.

## 2.3 Vibration-based Tests

In this study, the vibration-based experimental method is also adopted as an alternative strategy that indirectly measures the tangential interface stiffness from the dynamic properties of the system, i.e. the frequencies of vibration and the mode shapes. Figure 3a shows the experimental setup, which consists of two limestone specimens in dry contact, forming the interface under study. More specifically, the bottom specimen is glued on the ground, while a free-standing specimen is placed on top. The dynamic properties

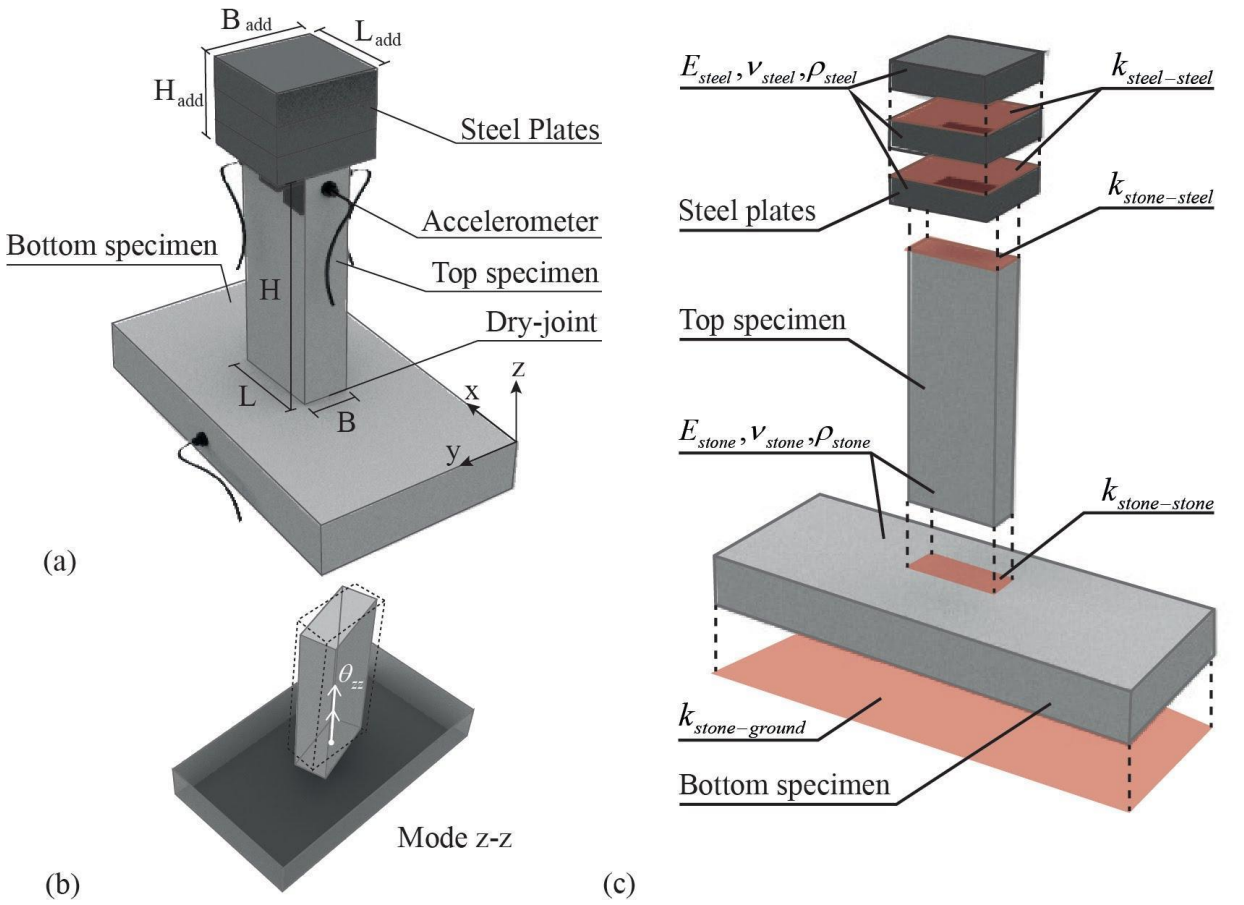


**Figure 3.** Vibration-based method: **(a)** experimental setup, **(b)** rotational mode shape over the z-z axis, and **(c)** schematic representation of the main components and mechanical parameters adopted in the numerical model

of the system are estimated through ambient dynamic identification, which presumes that the system undergoes perturbation of very low amplitudes, therefore allowing the use of linear dynamics. The tests are recorded using four accelerometers, three of them located on top of the top specimen (one in the x-x direction and two anti-diametrically placed in the y-y direction) and one on the bottom specimen (Figure 3a). The acquisition time of all the tests is 30 minutes with a sampling rate of 2000 Hz.

Furthermore, two different experimental setups are adopted. The first one focuses on the influence of the normal stress on the tangential interface stiffness, while the second one investigates the significance of the surface variability on the tangential interface stiffness. The first test setup uses five limestone specimens of dimension B=49.3 mm (CoV=0.3 %, N=5), L=151.0 mm (CoV=0.6 %, N=5), H=398.6 mm (CoV=0.1 %, N=5), progressively loaded by additional steel plates on top (Figure 3a). The top specimen is loaded up to a maximum of nine steel plates, each one having a mass equal to 10.51 kg and consequently allowing the maximum normal stress at the interface of 0.14 MPa. In the second instance, the setup includes 60 different top specimens of equal base dimension and variable height (section 2.1), which permits on one hand the investigation of the surface variability and on the other hand a small variation of normal stress at low ranges, i.e. from 0.004 MPa to 0.016 MPa.

The dynamic properties of the system are studied by employing the Enhanced Frequency Domain Decomposition (EFDD) method (Brincker et al. 1992, Magalhães et al. 2010). Figure 3b shows that the tangential interface stiffness can be correlated to the rotational mode of the top specimen over the z-z axis. After the estimation of the mode shape frequencies, the tangential interface stiffness is computed using inverse dynamic analysis with a finite element numerical model developed in the DIANA software (DIANA FEA 2021). More specifically, the numerical model reproduces the exact geometrical characteristics of the experimental setup (Figure 3c), while the mechanical properties used in the model are assumed considering a realistic range of values (Table 1). In particular, the tangential interface stiffness $k_{s,stone-stone}$ is calibrated by interpolating the experimental frequencies on the stiffness-frequency numerical results obtained by eigenvalue analyses. Furthermore, it is worth highlighting that previous (omitted herein for brevity) analyses demonstrated that all the rest of the mechanical parameters used do not influence the outcomes of the calibration process, since the rotational mode z-z (Figure 3b) is dictated by the tangential interface stiffness $k_{s,stone-stone}$.

**Table 1.** Mechanical properties of the flexible numerical model

| Element | Parameter | Reference |
|---|---|---|
| Limestone specimens | Elastic modulus $E_{stone}$ [GPa] | 32.7 |
| | Poisson's ratio $\upsilon_{stone}$ [-] | 0.2 |
| Stone-to-stone interface | Normal stiffness $k_{n,stone-stone}$ [MPa/mm] | $2 \cdot 10^1$ |
| | Tangential stiffness $k_{s,stone-stone}$ [MPa/mm] | calibrated |
| Stone-to-steel Interface | Normal stiffness $k_{n,stone-steel}$ [MPa/mm] | $1 \cdot 10^3$ |
| | Tangential stiffness $k_{s,stone-steel}$ [MPa/mm] | $5 \cdot 10^2$ |
| Steel-to-steel interface | Normal stiffness $k_{n,steel-steel}$ [MPa/mm] | $1 \cdot 10^5$ |
| | Tangential stiffness $k_{s,steel-steel}$ [MPa/mm] | $5 \cdot 10^4$ |
| Stone-to-ground interface | Normal stiffness $k_{n,stone-ground}$ [MPa/mm] | $1 \cdot 10^3$ |
| | Tangential stiffness $k_{s,stone-ground}$ [MPa/mm] | $5 \cdot 10^2$ |

# 3 Tangential Interface Stiffness

## 3.1 Deformation-based Results

Figure 4a illustrates two representative shear-box test results with a variation of the normal stress $\sigma_n$ applied at the joint, i.e. $\sigma_n$= 0.035 MPa and $\sigma_n$= 0.14 MPa. As expected, the response of the joint in both tests shows an initial elastic-stick phase, followed by the micro-slip and the gross-slip phases where sliding occurs (Fantetti et al. 2021). The comparison of the two tests indicates that the tangential interface stiffness increases with the normal stress. This is physically interpreted by the fact that higher normal stress results in a higher number of asperities in contact at the micro-scale.

Figure 4b collects the results of the tangential interface stiffness $k_s$ from all the shear-box tests against the normal stress $\sigma_n$. The tangential interface stiffness is estimated by the elastic-stick phase, using up to 50% of the sliding shear stress in order to avoid the influence of the micro-slip phenomena (Figure 4a). Once more, it is observed that $k_s$ increases with $\sigma_n$, in agreement with past studies (e.g. Berthoud and Baumberger (1998).

## 3.2 Vibration-based Results

Figure 5a presents the modal frequencies $f$, identified using the vibration-based tests, with respect to the normal stress $\sigma_n$ acting on the interface. The variation of $\sigma_n$ is achieved by varying either the slenderness (i.e. aspect ratio) of the specimens or the steel plates (section 2.3). As expected, Figure 5a shows a decrease in the frequency with the increase of mass, which also results in the increase of the normal stress at the interface. Employing the methodology described in section 2.3, Figure 5b converts the experimentally measured frequencies $f$ of Fig. 5a into values of tangential interface stiffness $k_s$. Overall, Figure 5b shows that $k_s$ increases with $\sigma_n$, similarly to the deformation-based tests (section 3.1).

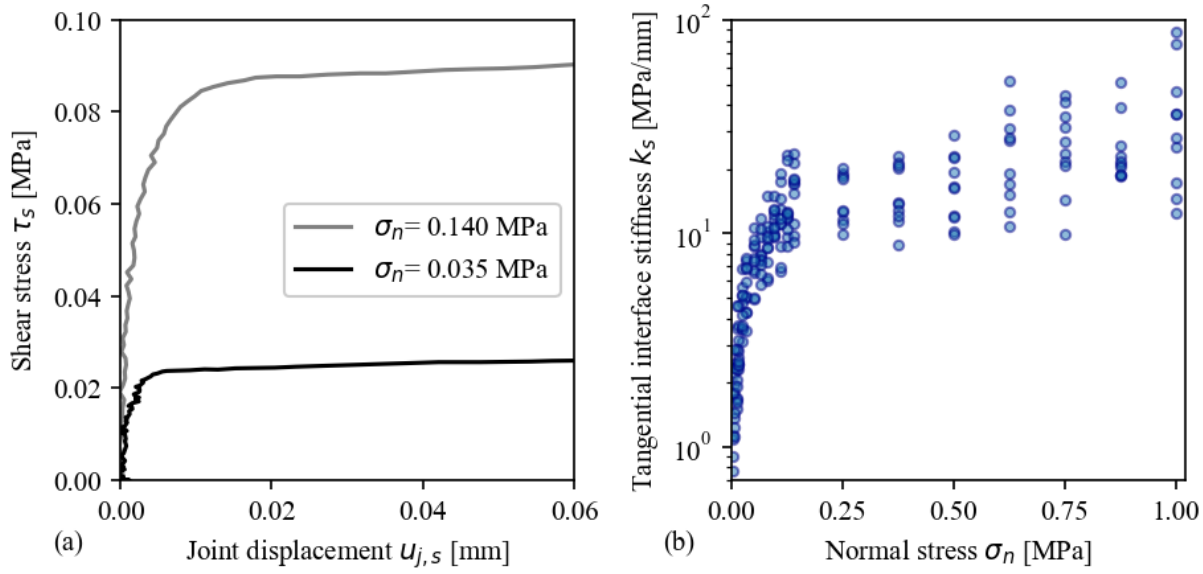


**Figure 4. (a)** Two representative shear-box test results with different normal stress (i.e. $\sigma_n$=0.035 MPa and $\sigma_n$=0.14 MPa), and **(b)** tangential interface stiffness $k_s$ against the normal stress $\sigma_n$ obtained after all the shear-box tests

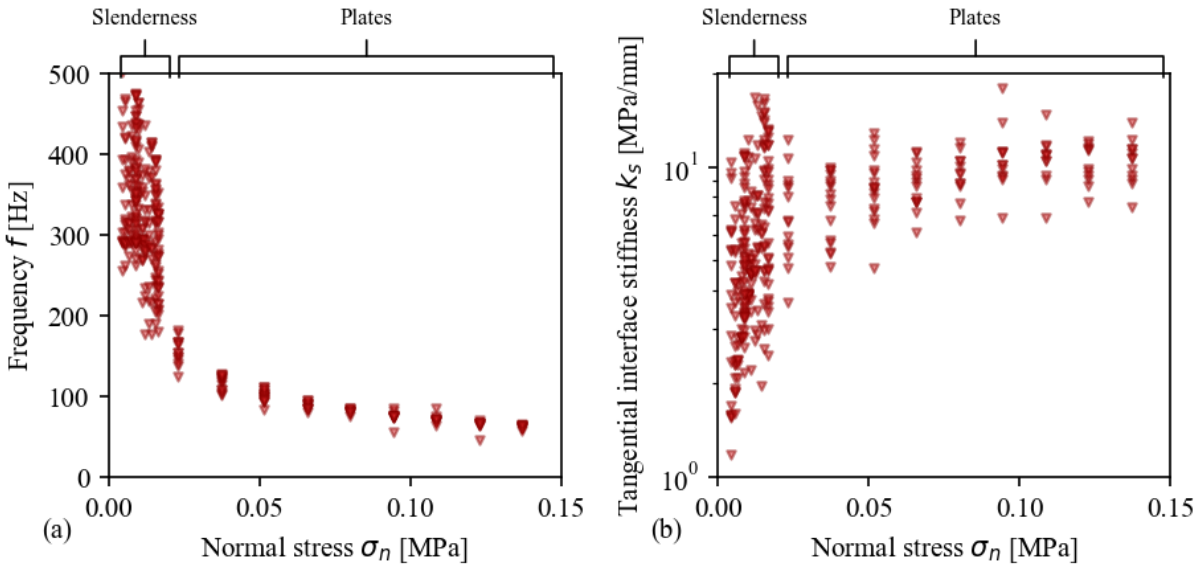


**Figure 5. (a)** Identified modal frequencies $f$ after the vibration-based tests, and **(b)** the corresponding tangential interface stiffness $k_s$

### 3.3 Comparison of Deformation-based and Vibration-based Results

The deformation-based and the vibration-based tests are two fundamentally different experimental methods for estimating the interface stiffness of dry-joints, thus, it is of paramount importance to compare and cross-validate their outcomes. Figure 6 summarizes the results of both methods in estimating the tangential interface stiffness $k_s$ (Figure 4b and Figure 5b) and shows a very good agreement between the deformation-based and vibration-based experimental methods, for the whole range of normal stress $\sigma_n$.

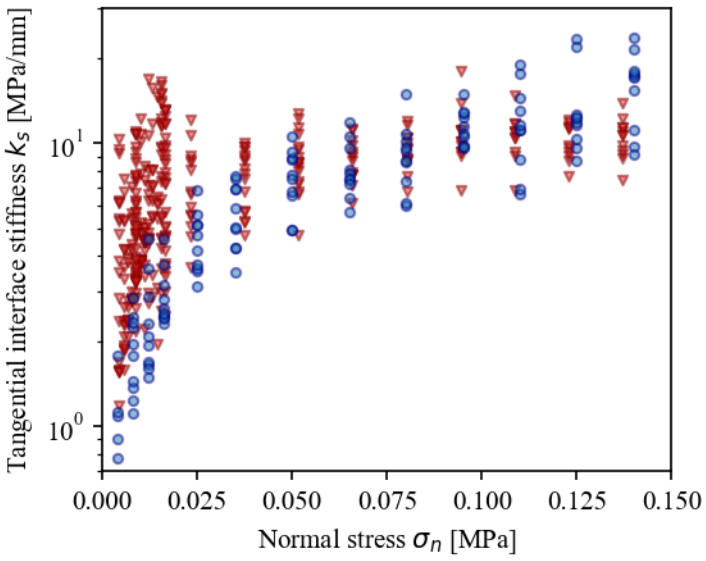


**Figure 6.** Comparison of the deformation-based and the vibration-based methods in estimating the tangential interface stiffness $k_s$

To the best of the author's knowledge, this is the first time that results from such inherently different experimental methods are successfully compared and cross-validated.

## 4 Conclusions

This work presents an extensive experimental campaign for the estimation of the tangential interface stiffness of dry-joint limestone specimens. To this aim, two fundamentally different experimental methods are employed and compared, namely deformation-based and vibration-based. The former quantifies the stiffness as the gradient of stress over the joint displacement upon loading, while the latter indirectly estimates the stiffness through the measurement of ambient vibrations related to the interface.

The results of the tests clearly indicate that the tangential interface stiffness increases together with normal stress acting at the interface. This is attributed to the increasing number of asperities in actual contact at the micro-scale of the interface. Furthermore, the outcomes of the two employed experimental methods have been successfully compared and cross-validated. This match enhances their reliability and at the same time demonstrates their possible alternative use.

Overall, it is worth highlighting that the presented experimental outcomes could be either employed directly by numerical and analytical models that simulate dry-joint masonry structures or form the basis for developing experimentally informed constitutive laws which consider this complex behavior.

## 5 Acknowledgments

This work has been partly financed by FCT/MCTES through national funds (PIDDAC) under the R&D Unit Institute for Sustainability and Innovation in Structural Engineering (ISISE), under reference UIDB/04029/2020. This work is financed by national funds through FCT - Foundation for Science and Technology, under grant agreements 2020.07325.BD and PRT/BD/152830/2021 attributed to the first and second authors, respectively.

This study has also been partly funded by the STAND4HERITAGE project (new STANDards FOR seismic assessment of built cultural HERITAGE) that has received funding from the European Research Council (ERC) under the European Union's Horizon 2020 research and innovation program (Grant No. 833123) as an Advanced Grant.

The opinions and conclusions presented in this paper are those of the authors and do not necessarily reflect the views of the sponsoring organizations.

The authors also greatly acknowledge the technical support from the staff of the University of Minho laboratory during the experimental campaign and Dr. Alberto Barontini from the University of Minho for the fruitful discussions and comments related to the vibration-based tests.

# 6 References


ASTM D7012-14E1. (2017). "Standard Test Methods for Compressive Strength and Elastic Moduli of Intact Rock Core Specimens under Varying States of Stress and Temperatures." American Society for Testing and Materials.

Baltazar, A., Rokhlin, S. I., and Pecorari, C. (2002). "On the relationship between ultrasonic and micromechanical properties of contacting rough surfaces." 50, 1397–1416.

Bandis, S., Lumsden, A. C., and Barton, N. R. (1983). "Fundamentals of Rock Joint Deformation." *International Journal of Rock Mechanics and Mining Sciences & Geomechanics Abstracts*, 20(6), 249–268.

Berthoud, P., and Baumberger, T. (1998). "Shear stiffness of a solid-solid multicontact interface." *Proceedings of the Royal Society A: Mathematical, Physical and Engineering Sciences*, 454(1974), 1615–1634.

Brincker, R., Krenk, S., Kirkegaard, P. H., and Rytter, A. (1992). "Identification of Dynamical Properties from Correlation Function Estimates." *Danish Society for Structural Science and Engineering.*, 63(1), 1–38.

Colombo, C., Savalle, N., Mehrotra, A., Funari, M. F., and Lourenço, P. B. (2022). "Experimental, numerical and analytical investigations of masonry corners: Influence of the horizontal pseudo-static load orientation." *Construction and Building Materials*, 344.

D'Altri, A. M., Sarhosis, V., Milani, G., Rots, J., Cattari, S., Lagomarsino, S., Sacco, E., Tralli, A., Castellazzi, G., and de Miranda, S. (2019). "Modeling Strategies for the Computational Analysis of Unreinforced Masonry Structures: Review and Classification." *Archives of Computational Methods in Engineering*, Springer Netherlands, 27, 1153–1185.

DIANA FEA. (2021). *User's Manual - Release 10.5*. DIANA FEA BV.

Drinkwater, B. W., Dwyer-Joyce, R. S., and Cawley, P. (1996). "A Study of the Interaction between Ultrasound and a Partially Contacting Solid--Solid Interface." *Proceedings of the Royal Society of London. Series A: Mathematical, Physical and Engineering Sciences*, 452(1955), 2613–2628.

Dwyer-Joyce, R. S., Drinkwater, B. W., and Quinn, A. M. (2001). "The use of ultrasound in the investigation of rough surface interfaces." *Journal of Tribology*, 123(1), 8–16.

Fantetti, A., Mariani, S., Pesaresi, L., Nowell, D., Cegla, F., and Schwingshackl, C. (2021). "Ultrasonic monitoring of friction contacts during shear vibration cycles." *Mechanical Systems and Signal Processing*, 161, 107966.

Filippi, S., Akay, A., and Gola, M. M. (2004). "Measurement of Tangential Contact Hysteresis During Microslip." *Journal of Tribology*, 126(3), 482–489.

Galvez, F., Sorrentino, L., Dizhur, D. Y., and Ingham, J. M. (2022). "Seismic rocking simulation of unreinforced masonry parapets and façades using the discrete element method." *Earthquake Engineering & Structural Dynamics*, 51(8), 1840–1856.

Gimpl, V., Fantetti, A., Klaassen, S. W. B., Schwingshackl, C. W., and Rixen, D. J. (2022). "Contact stiffness of jointed interfaces : A comparison of dynamic substructuring techniques with frictional hysteresis measurements." *Mechanical Systems and Signal Processing*, 171, 108896.

Kartal, M. E., Mulvihill, D. M., Nowell, D., and Hills, D. A. (2011). "Measurements of pressure and area dependent tangential contact stiffness between rough surfaces using digital image correlation." *Tribology International*, Elsevier, 44(10), 1188–1198.

Kim, J., Lorenzoni, F., Salvalaggio, M., and Rosa, M. (2021). "Seismic vulnerability assessment of free-standing massive masonry columns by the 3D Discrete Element Method." *Engineering Structures*, 246, 113004.

Kulatilake, P. H. S. W., Shreedharan, S., Sherizadeh, T., Shu, B., Xing, Y., and He, P. (2016).

"Laboratory Estimation of Rock Joint Stiffness and Frictional Parameters." *Geotechnical and Geological Engineering*, Springer International Publishing, 34(6), 1723–1735.

Magalhães, F., Cunha, Á., Caetano, E., and Brincker, R. (2010). "Damping estimation using free decays and ambient vibration tests." *Mechanical Systems and Signal Processing*, 24(5), 1274–1290.

Mulvihill, D. M., Brunskill, H., Kartal, M. E., Dwyer-joyce, R. S., and Nowell, D. (2013). "A Comparison of Contact Stiffness Measurements Obtained by the Digital Image Correlation and Ultrasound Techniques." *Experimental Mechanics*, 1245–1263.

Pesaresi, L., Fantetti, A., Cegla, F., Salles, L., and Schwingshackl, C. W. (2020). "On the Use of Ultrasound Waves to Monitor the Local Dynamics of Friction Joints." *Experimental Mechanics*, 60, 129–141.

Roca, P., Lourenço, P. B., and Gaetani, A. (2019). *Historic Construction and Conservation: Materials, Systems and Damage*. Routledge Taylor & Francis Group, New York.

Al Shawa, O., De Felice, G., Mauro, A., and Sorrentino, L. (2012). "Out-of-plane seismic behaviour of rocking masonry walls." *Earthquake Engineering & Structural Dynamics*, 41(5), 949–968.

Shi, X., and Polycarpou, A. A. (2005). "Measurement and Modeling of Normal Contact Stiffness and Contact Damping at the Meso." *Journal of Vibration and Acoustics*, 127(1), 52–60.

Sorrentino, L., Cattari, S., da Porto, F., Magenes, G., and Penna, A. (2019). "Seismic behaviour of ordinary masonry buildings during the 2016 central Italy earthquakes." *Bulletin of Earthquake Engineering*, Springer Netherlands, 17(10), 5583–5607.

Vlachakis, G., Giouvanidis, A. I., Mehrotra, A., and Lourenço, P. B. (2021). "Numerical block-based simulation of rocking structures using a novel universal viscous damping model." *Journal of Engineering Mechanics*, 147(11), 04021089.

Vlachakis, G., Vlachaki, E., and Lourenço, P. B. (2020). "Learning from failure: Damage and Failure of Masonry Structures, after the 2017 Lesvos Earthquake (Greece)." *Engineering Failure Analysis*, 117, 104803.

Zhao, G., Xiong, Z., Jin, X., Hou, L., and Gao, W. (2018). "Prediction of contact stiffness in bolted interface with natural frequency experiment and FE analysis." *Tribology International*, 127, 157–164.